RAPID COMMUNICATION

On the possibility of a new multiband heterostructure at the atomic limit made of alternate CuO_2 and FeAs superconducting layers

A Ricci[1], B Joseph[1], N Poccia[1], W Xu[2], D Chen[2], W S Chu[2], Z Y Wu[2,3], A Marcelli[4], N L Saini[1] and A Bianconi[1]

[1] Dipartimento di Fisica, Università di Roma 'La Sapienza', Piazzale Aldo Moro 2, 00185 Roma, Italy

[2] BSRF, Institute of High Energy Physics, Chinese Academy of Sciences, 10049, Beijing, People's Republic of China

[3] NSRL, University of Science and Technology of China, Hefei 230026, People's Republic of China

[4] INFN—Laboratori Nazionali di Frascati, Via E Fermi 40, 00044 Frascati, Rome, Italy

Abstract

Here we provide the material design of a possible high temperature multiband superconductor (HTMS) made of a 'heterostructure at the atomic limit' formed by alternate layers of electron doped FeAs and CuO_2 separated by intercalated NdO spacers. This new class of materials is derived from the two well known electron doped superconductors Nd_2CuO_4 and NdOFeAs belonging to the cuprate and the pnictide families, respectively. The calculated local electronic density of states show that both the Cu and Fe bands cross the Fermi surface. This will provide (i) superconducting Fermi arcs made by charges from the CuO_2 plane, and (ii) tubular Fermi surfaces, as in pnictides, by itinerant charges from the Fe atomic layer. The electronic properties of this new class of materials are presented to highlight the possibility of material design of a HTMS tuned at a shape resonance in the energy gap parameters belonging to the class of Fano–Feshbach resonances called superstripes. The Nd L_3-edge x-ray absorption near edge structure (XANES) of the proposed model system is calculated and compared with the XANES spectra of the Nd_2CuO_4 and NdOFeAs parent compounds.

(Some figures in this article are in colour only in the electronic version)

The recent discovery of high temperature multiband superconductivity (HTMS) in iron based compounds [1–12] has provided additional support for proposals focusing on exchange-like interband paring as the driving mechanism for high temperature superconductivity [13, 14]. In fact the new superconducting iron-pnictide materials show four key features predicted by these models: (i) they are made of multilayers, (ii) they are multiband metals, (iii) the Fermi level of these systems is near an 'electronic topological transition' (ETT) and (iv) they are multigap superconductors. Following these proposals, called the 'superstripes scenario', amplification of the superconducting critical temperature T_c occurs in systems with a material architecture made of 'metallic heterostructures at the atomic limit' [15, 16]. These are superlattices of superconducting units (layers, or stripes, or wires, or spheres or balls) separated by an intercalated material [17–20]. The electronic structure of such a system is made of multiple bands crossing the Fermi level with different symmetry and with projected partial density of states (PDOS) in different spatial locations of the heterostructure. The chemical potential
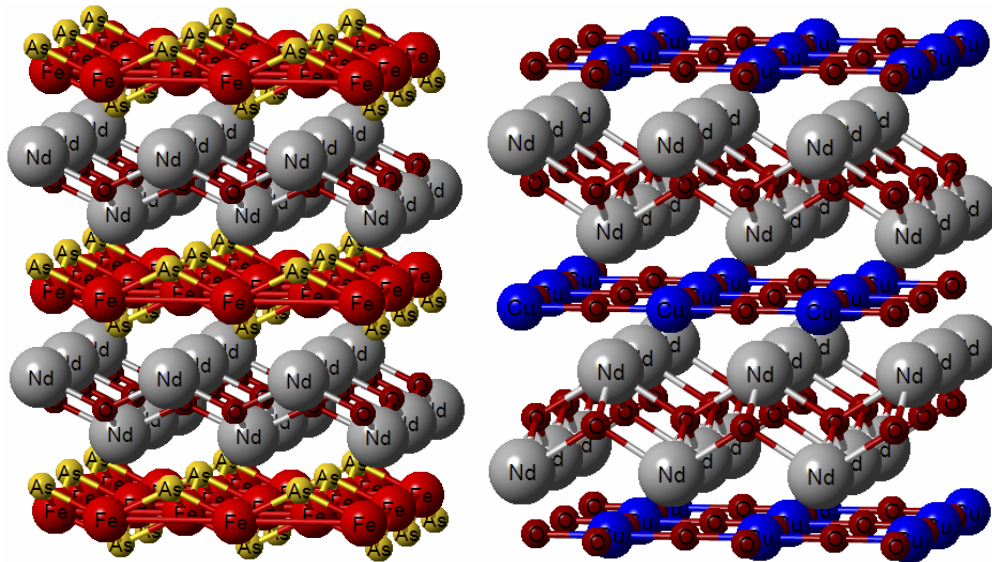
Figure 1. Crystal structure of NdOFeAs (left) and Nd_2CuO_4 (right). Superconducting Fe (in NdOFeAs) and CuO_2 (in Nd_2CuO_4) layers are intercalated by the same NdO fluorite spacer layers.

appears to be tuned (by changing the structure or the charge density) in the proximity of an ETT where one of the Fermi surfaces changes its topology and/or dimensionality. Finally in this regime a key term is the exchange-like term, called interband pairing, i.e. the exchange of pairs between condensates with different order parameters in bands with different symmetries and localization. This term controls the quantum interference between different pairing channels and could be the driving force for a shape resonance or Feshbach resonance [21] that pushes up the critical temperature. However, this regime is difficult to realize since the system near an ETT is on the verge of a catastrophe due to first order transitions triggered by impurities and disorder. Therefore in all known HTMS the shape resonance near the ETT shows up with a complex heterogeneity due to frustrated or complex phase separation. According to one of the many proposals, high T_c superconductivity by the amplification of the critical temperature has been associated mainly with a material architecture consisting of a 'heterostructure at the atomic limit' and tuning of the chemical potential by changing the lattice or the charge density [16, 22]. In this proposal the essential point for high T_c superconductivity is not the proximity to a Mott insulator, but the material architecture that is postulated to be an intrinsic feature. The discovery of superconducting diborides in 2001 [23] provided the first support for this model [24, 25]. In fact the diboride systems share a similar 'heterostructure at the atomic limit' with cuprates; a superlattice of quantum wells, where the superconducting atomic boron layers replace the quite different superconducting CuO_2 layers, and the metallic Mg spacers replace the complex spacers in the cuprates. The discovery of superconducting pnictides in 2008 [1] has provided further strong supporting for this proposal [26]. In fact pnictides have a very similar 'heterostructure at the atomic limit' architecture to cuprates; a superlattice of quantum wells, where the superconducting atomic FeAs layers replace the quite different superconducting CuO_2 layers and the REO (RE = rare-earth)

spacers in 1111 families replace the complex spacers in the cuprates.

The remarkable structural similarity of the cuprates and pnictides, from the functional point of view, can be easily visualized by considering the examples of NdOFeAs and Nd_2CuO_4 structures (figure 1). Both NdOFeAs and Nd_2CuO_4 have tetragonal symmetry at room temperature with similar lattice parameters. The NdO spacer layer is identical in both systems (figure 1). While the superconducting FeAs layers with reversed fluorite structure appear to be quite different from bcc CuO_2 layers, from the point of view of electronic transport, these two have identical roles to play. The 'heterostructures at the atomic limit' are characterized, first, by charge transfer between the superconducting layers and the spacers and, second, by the superlattice misfit strain [27–30]. The NdOFeAs and Nd_2CuO_4 are kinds of model systems where the superlattice misfit strain seems to play an important role in the superconducting properties. Both these systems become superconductors by charge transfer of electrons from the spacer to the superconducting layers. In both systems the NdO fluorite layers are under a compressive microstrain due to the superlattice misfit strain. Also in both, the superconducting planes, Fe and CuO_2 in the pnictide and cuprate systems, respectively, are under a tensile microstrain that favors electron doping. The compressive microstrain in the NdO fluorite layers allows the formation of oxygen ion vacancies that can also provide electronic charge transfer to the superconducting plane in the fluorite spacer layer. Both systems show interesting magnetic phase transitions. However, unlike NdOFeAs, Nd_2CuO_4 shows no structural phase transition and continues to be in the tetragonal phase even at low temperature, which is also found to be true for the doped compounds ($Nd_{1.85}Ce_{0.15}CuO_4$, and $Nd_{1.85}Ce_{0.15}CuO_{3.965}$) [31].

In this work we propose a possible new class of materials made of composite heterostructures where both CuO_2 and FeAs layers are embedded in the same superlattice. Figure 2 provides the model crystal structure of such a system,
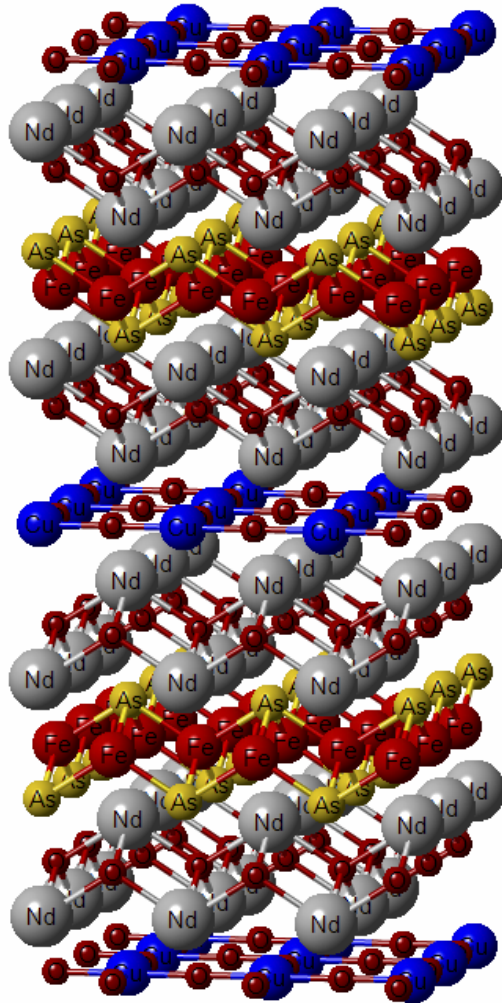
Figure 2. Structure of the $Nd_4CuO_6Fe_2As_2$ system formed by combination of CuO_2 and FeAs layer units intercalated by NdO fluorite layers.

Figure 3. The site projected density of states (PDOS) of the $Nd_4CuO_6Fe_2As_2$. Legends show the color code used for the different orbitals. The vertical dotted line indicate the position of E_F.

Table 1. Crystallographic parameters of the $Nd_4CuO_6Fe_2As_2$ system formed by combination of CuO_2, and FeAs layer units intercalated by NdO fluorite layers. Space group: $I4/mmm$, $a = b = 3.96$ Å, $c = 21$ Å. Crystallographic data corresponding to NdOFeAs and Nd_2CuO_4 are given in [32, 33]. As can be seen, the crystallographic structure of the new compound is similar to the parent compounds, which is expected due to the striking structural similarity between the two systems (figure 1).

Atom type	x	y	z
Nd	0	0	0.17
Nd	0	0	0.57
O	0	0.5	0
O	0	0.5	0.62
Cu	0	0	0
Fe	0	0.5	0.25
As	0	0	0.30

$Nd_4CuO_6Fe_2As_2$. Table 1 presents the crystallographic details of this structure. The NdO spacer layer in this new superlattice structure separates two different kinds of charge-carrier layer either side. This implies that from the electronic structure point of view, the Nd atoms are going to have two distinct sites (electronically, two distinct PDOS for a Nd atom depending on its site). This new class of 'heterostructures at the atomic limit' could provide a very exciting HTMS made of CuO_2 and FeAs superconducting layers with different superconducting gaps in the different layers and a single superconducting critical temperature controlled by proximity effects, i.e. the interband exchange-like pairing interaction.

The PDOS of the constituent elements of the $Nd_4CuO_6Fe_2$ As_2 system is shown in figure 3. The PDOS calculation method is described in a recent article [34]. As expected from the Nd_2CuO_4 and NdOFeAs electronic structure, the near Fermi level (E_F) states in this case are also dominated by the d states of Cu and Fe. Importantly, as is evident from the Nd PDOS (upper two panels in figure 3), there is a relatively large weight for the Nd f states near the E_F for the two distinct Nd sites, albeit with a noticeable difference in the spectral
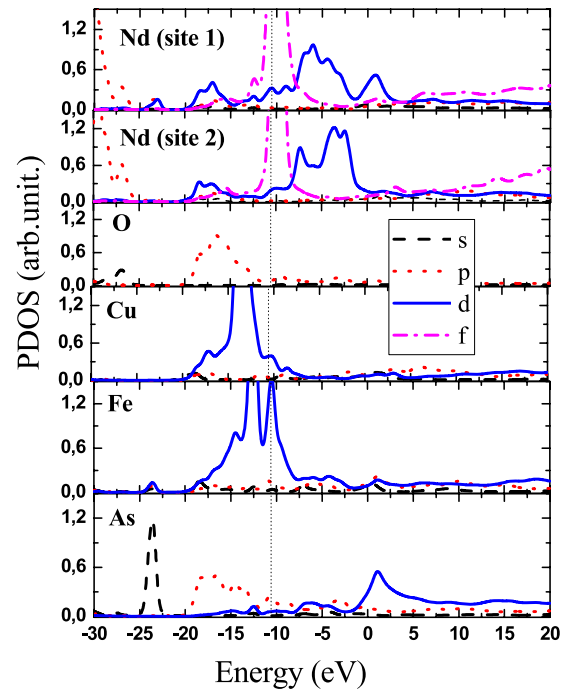
weight distribution. The Nd ground state is [Xe] $4f^46s^2$ with a partially filled 4f state. The d state also make a non-negligible contribution to the near E_F DOS, especially the unoccupied states close to E_F. From figure 3 it is evident that the major contribution to the near E_F DOS comes from Nd, Cu and Fe. The calculated PDOS shows that both Cu and Fe bands cross the Fermi surface. This will provide, first, superconducting Fermi arcs [35] made by charges from the CuO_2 plane and, second, tubular Fermi surfaces like in the pnictides [36, 37] made by itinerant charges in Fe atomic layer. It is interesting to compare how the electronic structure of these elements in the superstructure ($Nd_4CuO_6Fe_2As_2$) varies from that of the 'parent compounds (NdOFeAs and Nd_2CuO_4)'. For that purpose, in figure 4, we plot the PDOS of these elements in the 'superstructure' and 'parent compounds'.
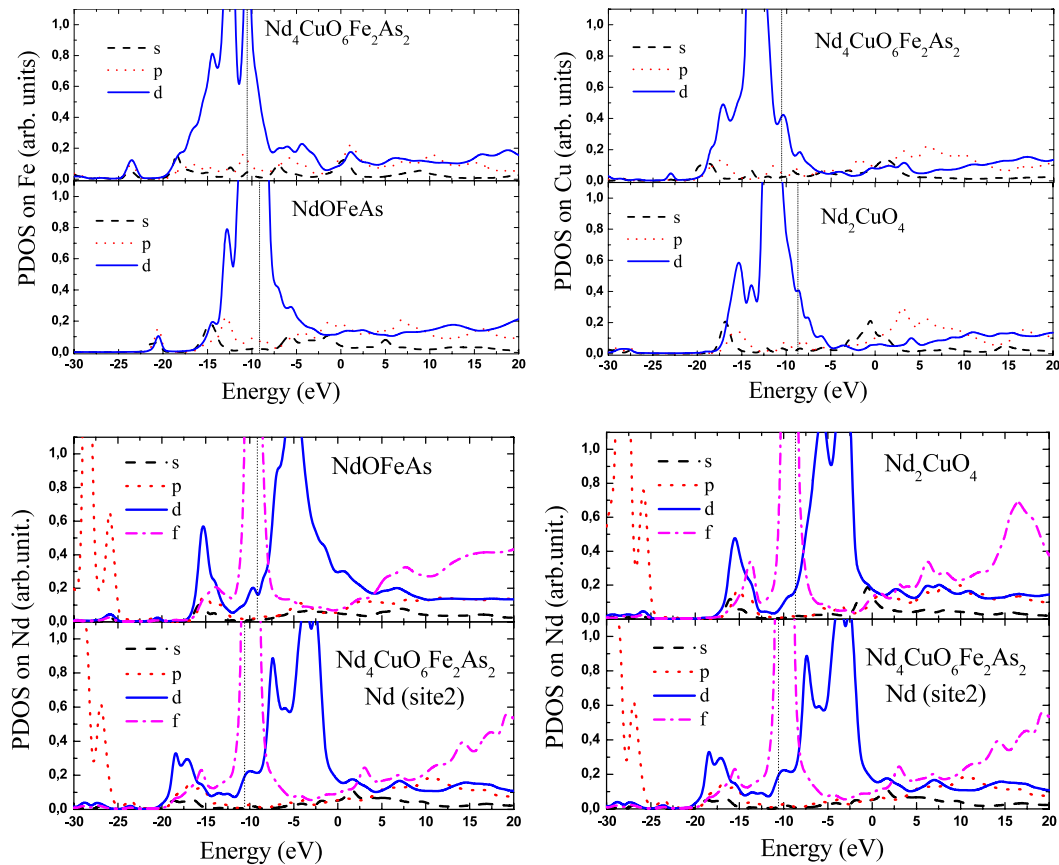
Figure 4. Comparison of the PDOS of $Nd_4CuO_6Fe_2As_2$ with its parent phase compounds NdOFeAs and Nd_2CuO_4. Upper right and lower right panels compare, respectively, the Fe PDOS and the Nd PDOS of the NdOFeAs and $Nd_4CuO_6Fe_2As_2$ systems. Upper left and lower left panels compare, respectively, the Cu PDOS and the Nd PDOS of the Nd_2CuO_4 and $Nd_4CuO_6Fe_2As_2$ systems. The dotted line in all panels indicates the position of E_F.

The d states of Cu and Fe are the key players in the quasiparticle formation of the cuprate [35] and pnictide [36, 37] systems, respectively. A comparison of these d states in the 'parent phase' with that of the superstructure reveals substantial changes in its near E_F spectral weights (figure 4). From the structural point of view, the origins of such differences are not so evident. Looking back at the structure (figures 1 and 2), from the Fe site, the Fe–As charge-carrier layer in NdOFeAs and $Nd_4CuO_6Fe_2As_2$ have identical spacer layers (NdO) on both sides. The situation for the other charge-carrier layer, Cu–O, is similar. While these charge-carrier layers in the superstructure have identical near-neighbor environment as the parent compounds, the common spacer layer in the superstructure (NdO), sees completely different layers on both sides. This gives rise to two inequivalent sites for Nd, resulting in two different PDOS (denoted as Nd (site1) and Nd (site2) in figure 3). The changes seen in the PDOS of the 'active elements' (Cu and Fe), especially for the d orbitals, of the superstructure in comparison with the 'parent phase' clearly reveals that the properties of the former are not going to be a simple superposition of the properties of the constituent parent phases. This clearly underlines the importance of the practical realization of such a system. It should be mentioned that in an experimental realization of such a superstructure, it is very probable that the structural parameters could also be modified slightly, leading to changes

in the electronic structure. Alternatively, there could also be slight changes occurring in the structure due to changes in the electronic bands as a result of proximity effects. In an interesting resonant x-ray spectroscopy study on the interface between high temperature superconducting $(Y, Ca)Ba_2Cu_3O_7$ and metallic $La_{0.67}Ca_{0.33}MnO_3$, Chakhalian *et al*, showed the importance of orbital reconstruction and covalent bonding in designing of oxide heterostructures with engineered physical properties [38]. It is found that a charge of about -0.2 electron is transferred from Mn to Cu ions across the interface, resulting in a major reconstruction of the orbital occupation and orbital symmetry of the CuO_2 layers. In the present case, although the active layers, CuO and FeAs, are separated by the identical NdO spacer layer, a coupling between the active layers, especially when the spacer layer is in the doped condition, can have non-trivial consequences for the functional properties of the system.

Having calculated the electronic structure, it is tempting to make use of the above in performing possible comparisons with available experimental data. Comparison with the x-ray absorption data is one way to do that. This also helps in further clarifying the electronic and structural correlations. We have used the Nd L_3-edge XANES data for this purpose. In figure 5, we present the normalized experimental and calculated XANES spectra of the NdOFeAs and Nd_2CuO_4 systems. The experimental data for the Nd_2CuO_4 are taken
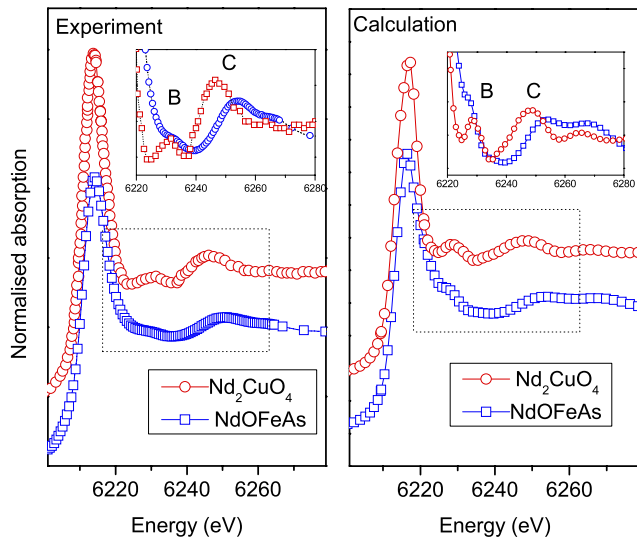
Figure 5. Comparison of Nd L_3 XANES spectra from Nd_2CuO_4 and NdOFeAs. Experimental data are shown in the right panel and the corresponding FEFF calculation results are shown in the left panel. The inset shows zoomed view of the near-edge features.

Figure 6. Effect of unit-cell compression on the calculated Nd_2CuO_4 XANES spectra in comparison with that of NdOFeAs. The right panel shows the zoomed view of the near-edge features of Nd_2CuO_4 upon compression. A 3% compression of the Nd_2CuO_4 gives reasonable matching of the near-edge features of this with that of NdOFeAs.

from [39] while those for NdOFeAs are taken from [40]. Both the spectra show an intense peak, the characteristic white line (WL) of Nd^{3+}. It is worth recalling that the L_3 absorption process is a $2p_{3/2} \rightarrow 5\varepsilon d$ (or $2p_{3/2} \rightarrow 6\varepsilon s$) transition governed by the dipole selection rules ($l = \pm1$) and hence empty states with d or s symmetries (and admixed states) can be reached in the final state. Since the probability for a $2p_{3/2} \rightarrow 6\varepsilon s$ transition is about two orders of magnitude lower than for a $2p_{3/2} \rightarrow 5\varepsilon d$ transition, the earlier can be ignored for describing the L_3 WL. The one-electron picture (i.e. all the orbitals not directly involved in the absorption process are passive in the final state) works well for the L_3 WL unless the materials of interest are mixed valence systems. In the present case, the WL appears to be typical of Nd^{3+} and hence the one-electron picture could be fairly used to describe the spectra. In addition to the intense WL, other predominant near-edge features observed are a weak structure around 15 eV above the WL (feature B), and the continuum resonances appearing as a two peak structure (feature C). Interestingly, the 1111-pnictide systems show a systematic variation of the energy difference between the WL and the continuum resonance features in accordance with the REO and REA distances [40]. The slight shift in the continuum resonance peak towards the lower energy in the case of Nd_2CuO_4 is consistent with the slightly increased distance of the NdO bond length in this case. These results are in line with the $\Delta E \propto 1/d^2$ rule for multiple scattering resonances [41]. The XANES simulations over the Nd-L_3 edge were performed using self-consistent real-space multiple scattering calculations using the FEFF8.2 code [42, 43] within the muffin-tin approximation. The atomic potential is calculated self-consistently using a cluster of radius 8.0 Å. For the calculations, the energy and position dependent Hedin–Lundqvist optical potential [44] has been selected as the exchange–correlation potential. The total electronic potential was constructed by spherically averaging
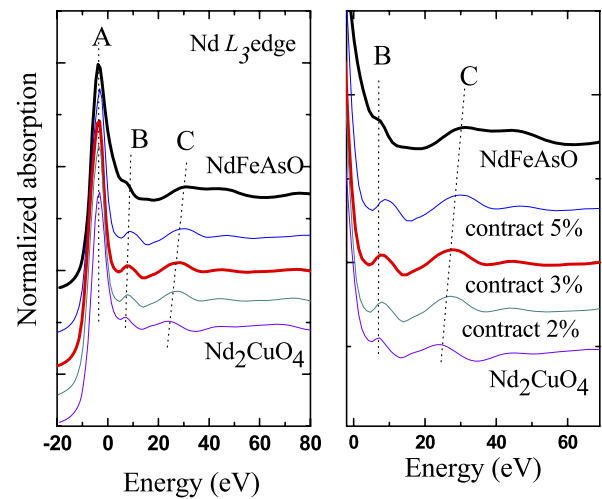
the muffin-tin potentials on each atom and keeping constant the potential in the interstitial region between the muffin-tin spheres. The f states of the Nd were kept frozen to achieve convergence of the self-consistent potential.

The XANES calculations show overall agreement with the experimental data for both the NdOFeAs and Nd_2CuO_4 systems (figure 5). However, a detailed comparison (inset figure 5) indicates a difference in the amplitudes of the different near-edge features, especially the feature B. It should be recalled that a similar feature B has been detected in the L_3-edge XANES spectra of different cuprate compounds, but discussion of this feature in the past was limited to the structural symmetries [39, 45–47]. With the appearance of iron-pnictide superconductors, such a feature in the rare-earth L_3-XANES spectra again come to light. In the REOFeAs system, it is observed that feature B changes systematically with the rare-earth size [40]. Comparison with multiple scattering calculations and the experimental data revealed that feature B has both a local structural and an electronic origin [34]. As discussed earlier, although the NdOFeAs and Nd_2CuO_4 share identical crystal configurations, with similar layer structures (figure 1), a good overlap of the XANES features is not seen in either the experimental or theoretical calculations (figure 5). In order to check the possible role of the difference in the lattice constants of the two systems in the above, we have studied the effect of compression of the Nd_2CuO_4 unit-cell on its XANES spectrum in comparison with that of the NdOFeAs. Results of such a study are presented in figure 6.

A 3% compression of the Nd_2CuO_4 unit-cell gives reasonable matching of the near-edge XANES features of this with that of NdOFeAs. Looking at the evolution of the near-edge features (figure 6 left panel), it is evident that feature B is also influenced by the unit-cell compression. The continuum resonance peaks also show the expected shift towards higher
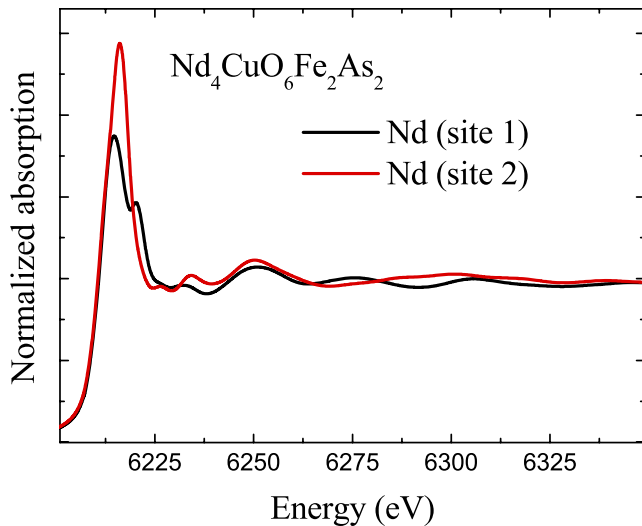
Figure 7. FEFF calculation results for the Nd L_3 XANES spectra from the two Nd sites in $Nd_4CuO_6Fe_2As_2$.

energy with the shorter unit-cell following the $\Delta E \propto 1/d^2$ empirical rule [41]. In fact, such a small change in the lattice constants of the Nd_2CuO_4 was actually implemented in generating the superstructure shown in figure 2. This small but finite difference in the lattice constants of the two parent phases involved in the superstructure is a key ingredient for handling the misfit strain in such a system. In addition, it also make the 'superstripes scenario' [20, 27, 29, 30] all the more interesting in such superstructures.

At this stage, it is also interesting to look into the Nd L_3-XANES spectrum of the $Nd_4CuO_6Fe_2As_2$ system. The FEFF calculation results for the Nd L_3-XANES spectra from the two Nd sites in $Nd_4CuO_6Fe_2As_2$ are shown in figure 7. As expected, the spectra from the two sites show different near-edge features. There is also a substantial difference in the WL intensities of the two components. From the experimental point of view, the Nd L_3-XANES spectrum of the $Nd_4CuO_6Fe_2As_2$ system should be similar to the average of the calculated spectra from the two Nd sites. A comparison of XANES spectra calculated for the NdOFeAs and Nd_2CuO_4 (figure 5) with that of the $Nd_4CuO_6Fe_2As_2$ (figure 7) shows that the latter has an entirely different near-edge structure, once again underlining the possibilities for manipulation of the electronic degrees of freedom of such superstructures, in addition to the microstrain engineering aspects.

Summary

Here we propose a novel class of heterostructures made of alternate layers of pnictides and cuprates to produce HTMS materials which have additional microscopic degrees of freedom. These HTMS are multilayers involving alternate layer components from cuprate and iron–arsenide superconductor families. In particular, we provide a specific example of a composite system involving two basic components, Nd_2CuO_4 and NdOFeAs. The idea of such a HTMS is motivated by the striking similarities in the structural and electronic (as evidenced by the Nd L_3-XANES) properties of the Nd_2CuO_4 and NdOFeAs systems. The electronic properties and the XANES calculations for this novel HTMS are presented to highlight the importance of such a superstructure which offers further scope for the material manipulation of high temperature superconductors.

Acknowledgments

References

[1] Kamihara Y, Watanabe T, Hirano M and Hosono H 2008 *J. Am. Chem. Soc.* **130** 3296
[2] Ren Z-A *et al* 2008 *Chin. Phys. Lett.* **25** 2215
[3] Zhi-An R *et al* 2008 *Europhys. Lett.* **83** 17002
[4] Chen G F, Li Z, Li G, Hu W-Z, Dong J, Zhou J, Zhang X D, Zheng P, Wang N L and Luo J-L 2008 *Chin. Phys. Lett.* **25** 3403
[5] Chen X H, Wu T, Wu G, Liu R H, Chen H and Fang D F 2008 *Nature* **453** 761
[6] De la Cruz C *et al* 2008 *Nature* **453** 899
[7] Chen G F, Li Z, Wu D, Li G, Hu W Z, Dong J, Zheng P, Luo J L and Wang N L 2008 *Phys. Rev. Lett.* **100** 247002
[8] Wang X C, Liu Q Q, Lv Y X, Gao W B, Yang L X, Yu R C, Li F Y and Jin C Q 2008 *Solid State Commun.* **148** 538
[9] Tapp J H, Tang Z, Lv B, Sasmal K, Lorenz B, Chu P C W and Guloy A M 2008 *Phys. Rev.* B **78** 060505
[10] Hsu F-C *et al* 2008 *Proc. Natl Acad. Sci. USA* **105** 14262
[11] Fang M H, Pham H M, Qian B, Liu T J, Vehstedt E K, Liu Y, Spinu L and Mao Z Q 2008 *Phys. Rev.* B **78** 224503
[12] Zhu X, Han F, Mu G, Cheng P, Shen B, Zeng B and Wen H-H 2009 *Phys. Rev.* B **79** 220512
[13] Bianconi A 2005 *J. Supercond.* **18** 25
[14] Kristoffel N, Rubin P and Ord T 2008 *J. Phys.: Conf. Ser.* **108** 012034
[15] Bianconi A 2001 *US Patent Specification* US6, 265, 019 B1 http://patft.uspto.gov/netacgi/nph-Parser?Sect2= PTO1&Sect2=HITOFF&p=1&u=/netahtml/PTO/ search-bool.html&r=1&f=G&l=50&d=PALL&RefSrch= yes&Query=PN/6265019
[16] Bianconi A 1994 *Solid State Commun.* **89** 933
[17] Bianconi A, Poccia N and Ricci A 2009 *J. Supercond. Novel Magn.* **22** 527
[18] Fratini M, Poccia N and Bianconi A 2008 *J. Phys.: Conf. Ser.* **108** 012036
[19] Annett J, Kusmartsev F and Bianconi A 2009 *Supercond. Sci. Technol.* **22** 010301
[20] Ricci A, Poccia N, Ciasca G, Fratini M and Bianconi A 2009 *J. Supercond. Novel Magn.* **22** 589
[21] Bianconi A 2006 *Phys. Status Solidi* **203** 2950
[22] Bianconi A, Valletta A, Perali A and Saini N L 1998 *Physica* C **296** 269
[23] Nagamatsu J, Nakagawa N, Muranaka T, Zenitani Y and Akimitsu J 2001 *Nature* **410** 63
[24] Bianconi A, Castro D D, Agrestini S, Campi G, Saini N L, Saccone A, Negri S D and Giovannini M 2001 *J. Phys.: Condens. Matter* **13** 7383
[25] Bussmann-Holder A and Bianconi A 2003 *Phys. Rev.* B **67** 132509
[26] Caivano R *et al* 2009 *Supercond. Sci. Technol.* **22** 014004
[27] Agrestini S, Saini N L, Bianconi G and Bianconi A 2003 *J. Phys. A: Math. Gen.* **36** 9133

[28] Bianconi A, Agrestini S, Bianconi G, Castro D D and
     Saini N L 2001 *J. Alloys Compounds* **317** 537
[29] Poccia N, Ricci A and Bianconi A 2010 *Adv. Condens. Matter
     Phys.* **2010** 261849
[30] Bianconi A, Saini N L, Agrestini S, Castro D D and
     Bianconi G 2000 *Int. J. Mod. Phys.* B **14** 3342
[31] Kim J S and Kvam E P 1997 *Physica* C **292** 203
[32] Fratini M *et al* 2008 *Supercond. Sci. Technol.* **21** 092002
[33] Mueller-Buschbaum H and Wollschlaeger W 1975 *Z. Anorg.
     Allg. Chem.* **414** 76
[34] Xu W, Marcelli A, Joseph B, Iadecola A, Chu W S,
     Di Gioacchino D, Bianconi A, Wu Z Y and Saini N L 2010
     J. Phys.: Condens. Matter **22** 125701
[35] Damascelli A, Hussain Z and Shen Z-X 2003 *Rev. Mod. Phys.*
     75 473
[36] Zabolotnyy Z B *et al* 2009 *Nature* **457** 569
[37] Singh D J, Du M H, Zhang L, Subedi A and An J 2009 *Physica*
     C **469** 886
[38] Chakhalian J, Freeland J W, Habermeier H U, Cristiani G,
     Khaliullin G, Van Veenendaal M and Keimer B 2007 *Science*
     318 1114

[39] Tan Z, Filipkowski M E, Budnick J I, Heller E K, Brewe D L,
     Chamberland B L, Bouldin C E, Woicik J C and Shi D 1990
     Phys. Rev. Lett. **64** 2715
[40] Joseph B, Iadecola A, Fratini M, Bianconi A, Marcelli A and
     Saini N L 2009 *J. Phys.: Condens. Matter* **21** 432201
[41] Bianconi A, Fritsch E, Calas G and Petiau J 1985 *Phys. Rev.* B
     32 4292
[42] Ankudinov A L, Ravel B, Rehr J J and Conradson S D 1998
     Phys. Rev. B **58** 7565
[43] Ankudinov A L, Nesvizhskii A I and Rehr J J 2003 *Phys. Rev.*
     B **67** 115120
[44] Hedin L and Lundqvist S 1970 *Solid State Physics* vol 23,
     ed D T Frederick Seiz and E Henry (New York: Academic)
     p 1
[45] Tan Z, Budnick J I, Luo S, Chen W Q, Cheong S W,
     Cooper A S, Canfield P C and Fisk Z 1991 *Phys. Rev.* B
     44 7008
[46] Tan Z, Heald S M, Cheong S W, Cooper A S and Budnick J I
     1992 *Phys. Rev.* B **45** 2593
[47] Wu Z, Benfatto M and Natoli C R 1998 *Phys. Rev.* B
     57 10336

7